

Photoluminescence of $\text{InAs}_{0.04}\text{P}_{0.67}\text{Sb}_{0.29}$

Gene Tsai, De-Lun Wang, and Hao-Hsiung Lin^{a)}Graduate Institute of Electronics Engineering and Department of Electrical Engineering,
National Taiwan University, Taipei 10617, Taiwan

(Received 3 March 2008; accepted 22 May 2008; published online 30 July 2008)

We report the results of a detailed photoluminescence (PL) study on quaternary $\text{InAs}_{0.04}\text{P}_{0.67}\text{Sb}_{0.29}$ grown by gas-source molecular-beam epitaxy. The main PL peak at 10 K shows a transition energy that is lower than the calculated energy gap by 0.223 eV, which is attributed to the tail states recombination. Another PL band, which emerges as the temperature increases, is assigned to the self-activated luminescence from defect centers. Its features, namely, nearly temperature-independent peak energy, Gaussian-like lineshape, and square-root-of-temperature-dependent linewidth, can be illustrated by the configuration coordinate model. The vibration energy, calculated from the linewidth at low temperature, is 0.022 eV for the excited state of the defect centers. The self-activated luminescence shows a thermal quenching behavior that is usually exhibited by amorphous semiconductors, indicating that the defects are related to the compositional disorder. The defects responsible for the luminescence are most likely complexes consisting of a substitutional carbon and an In vacancy. © 2008 American Institute of Physics. [DOI: 10.1063/1.2960504]

I. INTRODUCTION

Midinfrared (MIR) emitters covering the 2–4 μm spectral range have attracted much attention due to their promising applications in gas sensing or free-space communications.^{1,2} Previous studies revealed that InAsPSb quaternary lattice matched with InAs is a useful alloy for MIR emitters.^{3,4} However, a miscibility gap (MG) exists in the low-As side of InAsPSb , which limits the growth range and the usefulness of this alloy.⁵ Several works reported the growth of high-quality InAsPSb alloys with compositions close to the MG boundary by using liquid-phase epitaxy. The lowest As mole fraction achieved in these reports was ~ 0.36 , along with the successful demonstration of 2.5 μm light-emitting diodes.⁶ Metal-organic chemical vapor deposition and molecular beam epitaxy (MBE) are commonly considered to be far from thermal equilibrium. Their capability of growing InAsPSb lying deeply in the MG region have been demonstrated.^{7–9} In this respect, many studies were focused on the material growth of InPSb . Its application to the cladding layers of MIR laser devices was also reported.⁸ However, a systematic investigation into the optical properties of low-As InAsPSb is still required. So far, the most important finding on this issue is that the transition energy of the photoluminescence (PL) is much lower than the energy gap, which is due to the strong compositional disorder in the alloys.^{7,9} In this paper, we report a detailed study on the PL of an $\text{InAs}_{0.04}\text{P}_{0.67}\text{Sb}_{0.29}$ bulk layer. In addition to the band tail luminescence resulting from the compositional disorder, we observed self-activated luminescence. The luminescence shows a Gaussian-like lineshape, temperature-independent peak energy, and a linewidth proportional to the square root of the temperature. The intensity shows a temperature dependence that is usually exhibited by amorphous semiconduc-

tors, revealing that the defects are related to the compositional disorder. The origins of the luminescence are most likely due to complexes consisting of a substitutional carbon and an In vacancy.

II. EXPERIMENTAL PROCEDURES

A VG-V80H gas-source MBE (GSMBE) system was used to grow 1- μm -thick $\text{InAs}_{0.04}\text{P}_{0.67}\text{Sb}_{0.29}$ on a (100) *n*-type InAs substrate. Pure arsine (AsH_3) and phosphine (PH_3), the precursors of the two group-V gas sources, were cracked in a gas cell at 1000 °C to provide the As_2 and P_2 beams for the epitaxy process. A mixed beam of Sb_2 and Sb was supplied by a cracking effusion cell (EPI Inc.). A conventional thermal effusion cell was employed as the group-III (In) source. The beam fluxes of the Sb and In sources were calibrated using an ion gauge, while those of the As and P sources were controlled by the gas pressures of the arsine and phosphine in the manifolds behind the microleaks of the gas cell. The growth temperature was set at 470 °C and the growth rate was kept at 1 $\mu\text{m}/\text{h}$. After the growth, a JEOL JXA-8200 electron probe microanalyzer was used to quantify the composition of the InAsPSb epilayers. InAs , InP , and InSb binary substrates were used as standards for ZAF correction. PL measurements were carried out using a SPEX 500M monochromator calibrated by the radiation lines of a Xe lamp. The sample under test was excited by a 532 nm diode-pumped solid-state laser. The luminescence was first dispersed by the monochromator and then collected by a liquid-nitrogen-cooled InSb detector. In order to prevent the atmospheric absorption, particularly the absorption by water vapor at 2.7 μm , in this work, CaF_2 lenses and windows were used and nitrogen gas was used to purge the optical path and the monochromator.

^{a)}Electronic mail: hhlin@ntu.edu.tw.

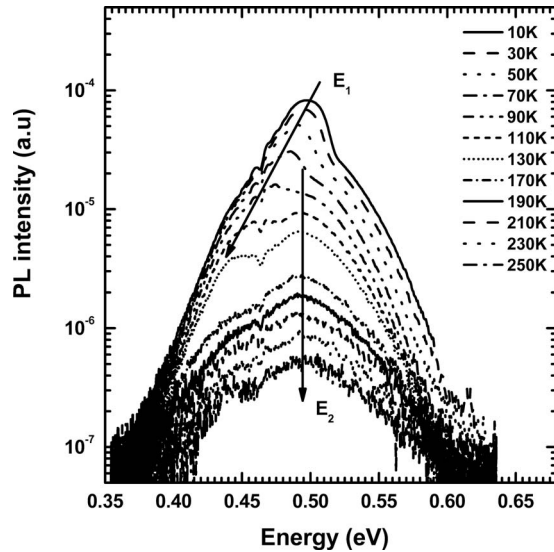


FIG. 1. Temperature-dependent PL spectra of $\text{InAs}_{0.04}\text{P}_{0.67}\text{Sb}_{0.29}$. The temperature range is 10–250 K. Peak E_1 redshifts as the temperature increases. Above 90 K, peak E_2 dominates the spectrum; its peak energy is independent of temperature.

III. RESULTS AND DISCUSSIONS

The composition of the studied sample, a 1- μm -thick $\text{InAs}_{0.04}\text{P}_{0.67}\text{Sb}_{0.29}$ epilayer grown at 470 °C, lies deeply inside the MG region. Its detailed structural properties have been previously reported and indicate that the sample suffers from strong compositional disorder.⁹ Figure 1 shows the temperature-dependent PL spectra with the temperature ranging from 10 to 250 K. The excitation power was 100 W/cm^2 . As can be seen in the figure, when the temperature exceeds 170 K, the luminescence shows a single broadband with a Gaussian-like lineshape. The dip in the emission spectrum at 0.45–0.46 eV is due to the absorption of light by water vapor. However, as the temperature is further decreased, a bump gradually rises from the low-energy shoulder of the broadband and finally dominates the luminescence at 10 K. The bump and the broadband are hereafter referred to as E_1 and E_2 , respectively. In order to discern E_1 from E_2 , we used a Gaussian function to fit E_2 and then recovered the lineshape of E_1 by subtracting the fitting curve from the measured spectrum. The results are shown in Fig. 2. As we can see, the Gaussian fitting is reasonably good. The recovered E_1 band shows dips in its low-energy tail, which are due to the absorption of light by water vapor and measurement errors. The peak energies of these two bands are then plotted against the temperature in Fig. 3. For comparison, the theoretically calculated energy gap as a function of temperature is also depicted (dashed line). The calculation considered three binary energy gaps¹⁰ and the bowing parameters of InAsSb ,¹¹ InAsP ,¹¹ and InPsb .⁷ We assumed that the bowing parameters are temperature independent. The peak energy of the E_1 band redshifts from 0.5 to 0.44 eV as the temperature increases from 10 to 130 K, while the peak energy of E_2 is virtually fixed at 0.49 eV throughout the whole temperature range. Both peak energies are far below the calculated energy gap, as can be seen in the figure. The energy difference between E_1 and the calculated energy gap at 10 K is as large

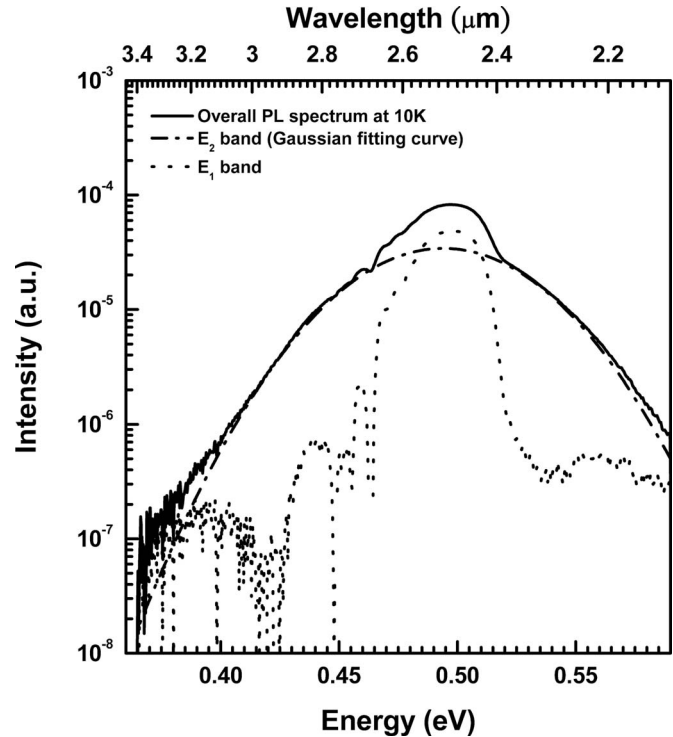


FIG. 2. Lineshape fitting for the 10 K PL spectrum. The overall spectrum can be decomposed into two bands. The broader E_2 band was obtained by Gaussian fitting and is attributed to deep-level transition. The stronger E_1 band was obtained by deducting the E_2 curve from the overall spectrum and is attributed to tail state transition. The dips around 0.45–0.46 eV in E_1 band are due to the absorption of light by water vapor, which is not considered in the Gaussian fitting. The deviation of the overall spectrum from the Gaussian fitting below the intensity level of 10^{-6} may have resulted from the measurement error and background noise.

as 0.223 eV. A similar phenomenon has been reported in literatures⁸ and was attributed to deep tail states resulting from compositional disorder.

Here, we ascribe the E_1 band to the recombination of the

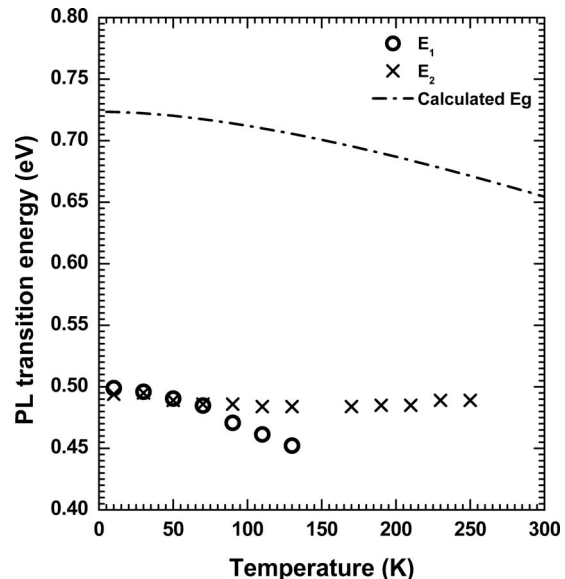


FIG. 3. PL transition energies as functions of temperature. Dashed line is the calculated band gap. The energy difference between the energy gap and E_1 transition energy is as large as 0.223 eV at 10 K.

carriers trapped in the deep tail states on the basis of the following observations. First, the E_1 band has a slow low-energy tail at 10 K, which is a feature of luminescence from tail states. Second, the peak energy is far below the calculated energy gap and agrees with the aforementioned findings in literatures.⁷ Moreover, we also performed power-dependent PL measurements at 10 K. The peak energy of the E_1 band retrieved from the overall spectrum shows a blueshift with increasing excitation power. Because of the low density of the band tail states, an increment in carrier density leads to filling of these states and results in the observed blueshift in the emission energy. The third observation is that the peak energy redshifts slightly faster than the calculated energy gap as the temperature increases, which indicates that the E_1 band is relevant to the energy bands. The faster slope is probably due to thermally assisted tunneling between the localized tail states. This tunneling process would allow the transition of carriers to lower energy states as the temperature increases and thus lead to a faster redshift. However, as we can see in Fig. 1, the increment in temperature also results in the diminishing intensity of the E_1 band. This implies that the carriers trapped in the tail states escape due to the thermal energy. Since the band edge luminescence at the calculated energy was not observed simultaneously, the escaping carriers are most likely recaptured by nonradiative centers either through extended bands or the tunneling process.

Because of its Gaussian-like lineshape, we attributed the E_2 band to the luminescence from a deep-level transition. Here, we use the configuration coordinate (CC) model to illustrate this recombination process.^{12,13} The model is generally applied to the defects with strong electron-phonon coupling. In such defects, the wave function of a trapped carrier is localized at a specific bond, and this asymmetrical distribution would induce the atoms to shift from their origin sites. After recombination, the atoms relax through lattice vibrations, i.e., the phonon emission process. Due to the parabolic nature of the energy versus position relation of lattice vibrations, the deep-level transition has a Gaussian-like lineshape, which is just the observed feature of the E_2 band. As can be seen in Fig. 3, the transition energy of the E_2 band is nearly independent of the temperature. This indicates that the luminescence is associated with a moleculelike defect center. If a defect center is sufficiently localized, the thermally induced lattice expansion and vibrations would almost exert no influence on its behavior; consequently, its luminescence peak energy would exhibit a negligible shift with temperature. This behavior has been reported in literatures and explained successfully by the CC model.¹³ To further confirm that the luminescence is from a defect, we inspect the temperature evolution of the full width at half maximum (FWHM) shown in Fig. 4. The FWHM derived from the CC model is given by

$$W = W_0[\coth(h\nu/2kT)]^{1/2}, \quad (1)$$

where $h\nu$ is the energy of the vibration mode of the excited state, kT is the thermal energy, and W_0 is the FWHM at 0 K, which is due to the minimum energy in quantum harmonic oscillators and can be expressed as follows:¹⁴

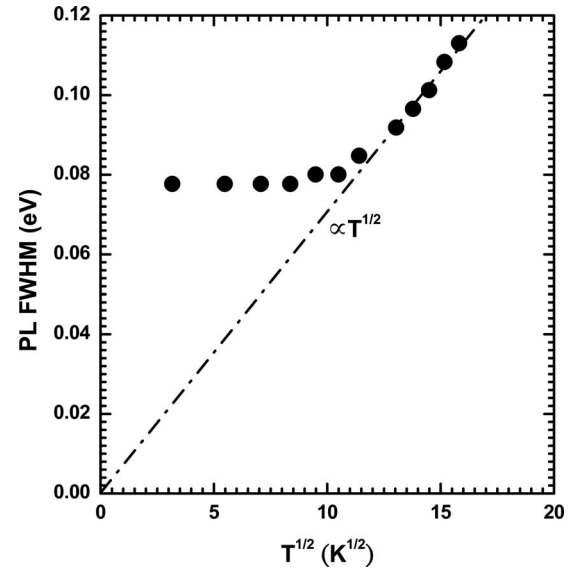


FIG. 4. FWHM of the PL band E_2 of $\text{InAs}_{0.04}\text{P}_{0.67}\text{Sb}_{0.29}$ as a function of the square root of temperature. In the high temperature range, FWHM fits the dashed line, indicating that it is proportional to the square root of temperature.

$$W_0 = (8S \ln 2)^{1/2} h\nu, \quad (2)$$

where S is the Huang–Rhys factor, which represents the mean number of phonon emissions. As can be seen in Fig. 4, the FWHM of the E_2 band satisfies Eq. (1) quite well. At high temperature, the FWHM is proportional to the square root of temperature. As the temperature is lower than 100 K, the FWHM saturates at 0.08 eV. From Fig. 4, one can find that $h\nu = 0.022$ eV, $W_0 = 0.08$ eV, and $S = 2.8$. The vibration energy of 0.022 eV is smaller but close to the energies of InSb-like longitudinal optical (LO) phonons in InPSb that is lattice-matched to InAs (0.024 eV).¹⁵ The small energy difference between the vibration mode and the InSb-like LO phonon mode of the host lattice implies that the Coulomb field induced by the defect charge has a slight effect on the lattice vibration, which explains the small Huang–Rhys factor.¹⁶

Figure 5 shows the integrated intensity of the E_2 band as a function of temperature. Here, instead of the Arrhenius plot, we adopt a formula, which has been used to consider the thermal quenching process in amorphous semiconductors,¹⁷ for the relation between the PL intensity I_{PL} and temperature T ,

$$I_{\text{PL}} = \frac{B}{1 + A \exp(T/T_0)}, \quad (3)$$

where T_0 is the characteristic temperature; A and B are constants. As can be seen, the equation is a fairly good fit to the integrated PL intensity with a characteristic temperature T_0 of 46 K. As the temperature increases, the local vibrations of the defect centers increase and eventually liberate the electrons in the excited states to the conduction band where they are lost by a nonradiative recombination process. Due to the compositional disorder in the sample, the defect centers at different locations have different activation energies, as shown in the inset of Fig. 5. Therefore, luminescence

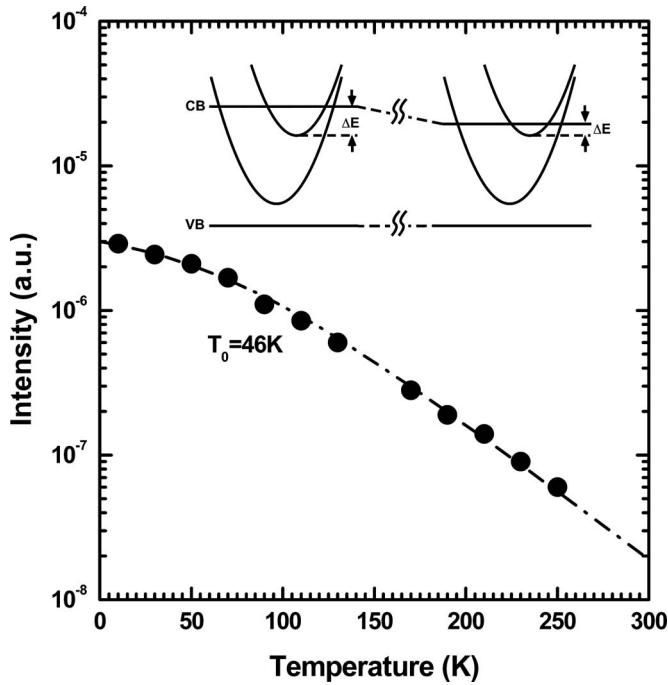


FIG. 5. Integrated PL intensity of the deep-level band E_2 as a function of temperature. Dashed line is the best fit of equation $I_{PL} = B/[1 + A \exp(T/T_0)]$, which is used to describe the quenching behavior of amorphous semiconductors. The inset shows the schematic CC diagrams of two defect centers at different locations. Due to the composition fluctuation, the defects see different conduction band edges and thus have different activation energies. The equation represents a collective quenching behavior of a group of defect centers with different activation energies.

quenching becomes a collective behavior of defect centers with different activation energies. Such a situation is similar to the conditions considered in the model proposed by Collins and Paul¹⁸ for amorphous Si:H, in which they suggested a distribution that represents the number of radiative centers with an activation energy of E ,

$$g(E) \propto \exp(-E/E_0), \quad (4)$$

where $E_0 = kT_0 \ln(C)$ and C is a constant relevant to the non-radiative recombination process. Here, because the change in activation energy is due to the composition fluctuation, E_0 is relevant to the variation in the conduction band seen by the defect centers. Reihlen *et al.*⁷ estimated E_0 in InPSb from below band edge absorption measurements. Their results were within 50–60 meV, much larger than $kT_0 \sim 4$ meV observed in this work. However, the absorption measurements were performed over the entire epilayer and hence correspond to the undulation of the energy gap of the entire sample. In contrast, the characteristic temperature T_0 observed from the quenching process in this study only represents the variation in the conduction band seen by the defects. Therefore, the large discrepancy between the results of Reihlen *et al.*⁷ and our results indicates that the defect centers are not uniformly distributed in the sample but concentrated in the potential wells resulting from the compositional disorder. The localization of the defects in a low-potential region may reduce the slope of the energy distribution seen by the defects, i.e., E_0 in Eq. (4). Such a defect distribution

implies that the defect centers could be generated by the compositional disorder.

The deep levels responsible for the E_2 band are possibly due to vacancy-impurity complexes. The nearly temperature-independent behavior of the E_2 peak energy suggests that the band is from a moleculelike center, which implies that both the ground and excited states should be within the energy gap. Pötz and Ferry¹⁹ have calculated the defect levels in III-V semiconductors using a rescaled defect-molecule model. However, the results for vacancies and antisites in InAs, InP, and InSb indicate that a single isolated defect cannot meet the requirements. We believe that the defect center is most likely composed of a substitutional carbon and an In vacancy, i.e., a $V_{In}-C_{As}$ or $V_{In}-C_{In}$ complex. Carbon is a common residual impurity in MBE-grown compound semiconductors. A few reports observed a carbon-related vibration gap mode at 220 cm^{-1} in carbon-doped InP grown by GSMBE and chemical beam epitaxy.^{20,21} The vibration energy of this mode is close to that of our sample. Moreover, in a previous study, Williams and Bebb¹⁴ observed the self-activated luminescence from a $V_{Ga}-C_{As}$ complex in GaAs. The reported vibration energy is also 0.022 eV.¹² Interestingly, the difference between the peak energy of $V_{Ga}-C_{As}$ complex and the energy gap is ~ 0.3 eV. Therefore, we attribute the E_2 band to the luminescence from complexes that consist of a substitutional carbon and an In vacancy. However, further research is required to understand the origin of the observed deep-level transition in InAsPSb.

IV. CONCLUSION

We report the results of a detailed PL study on an $\text{InAs}_{0.04}\text{P}_{0.67}\text{Sb}_{0.29}$ epilayer grown on an InAs substrate by GSMBE. Two PL bands were observed. The first one, dominant at 10 K, is attributed to the recombination of carriers trapped in the tail states resulting from compositional disorder. Its peak energy is lower than the calculated energy gap by 0.223 eV, indicating strong disorder in the alloy. Another PL band with Gaussian-like lineshape, dominant at higher temperature, is ascribed to a deep-level transition because its luminescence behaviors coincide with the signature of the CC model. The transition energy fixed at ~ 0.5 eV is virtually temperature independent. The vibration energy for the excited state is calculated from the linewidth and is 0.022 eV. The PL intensity shows a thermal quenching behavior that is usually exhibited by amorphous Si:H, revealing that the luminescence center is related to the compositional disorder. We believe that the origins of the luminescence are complexes consisting of a substitutional carbon and an In vacancy.

ACKNOWLEDGMENTS

This work was supported by the National Science Council of Taiwan under Grant No. NSC96-2221-E-002-279-MY3.

¹J. Wagner, C. H. Mann, M. Rattunde, and G. Weimann, *Appl. Phys. A: Mater. Sci. Process.* **78**, 505 (2004).

²M. Yin, A. Krier, S. Krier, R. Jones, and P. Carrington, *Proc. SPIE* **6399**, 63990C (2006).

- ³N. Kobayashi and Y. Horikoshi, *Jpn. J. Appl. Phys.* **19**, L641 (1980).
- ⁴H. Mani, E. Tournie, J. L. Lazzari, C. Alibert, and A. Joullie, *J. Cryst. Growth* **121**, 463 (1992).
- ⁵T. Fukui and Y. Horikoshi, *Jpn. J. Appl. Phys.* **20**, 587 (1981).
- ⁶A. Krier and Y. Mao, *IEEE Proc.: Optoelectron.* **144**, 355 (1997).
- ⁷E. H. Reihlen, M. J. Jou, Z. M. Fang, and G. B. Stringfellow, *J. Appl. Phys.* **68**, 4604 (1990).
- ⁸R. M. Biefeld, K. C. Baucom, S. R. Kurtz, and D. M. Follstaedt, *J. Cryst. Growth* **133**, 38 (1993).
- ⁹G. Tsai, D. L. Wang, C. E. Wu, C. J. Wu, Y. T. Lin, and H. H. Lin, *J. Cryst. Growth* **301–302**, 134 (2007).
- ¹⁰V. Swaminathan and A. T. Macrander, *Materials Aspects of GaAs and InP Based Structures* (Prentice-Hall, New Jersey, 1991), p. 10.
- ¹¹M. P. C. M. Krijn, *Semicond. Sci. Technol.* **6**, 27 (1991).
- ¹²F. E. Williams and M. H. Hebb, *Phys. Rev.* **84**, 1181 (1951).
- ¹³S. Shionoya, T. Koda, K. Era, and H. Fujiwara, *J. Phys. Soc. Jpn.* **19**, 1157 (1964).
- ¹⁴E. W. Williams and H. B. Bebb, in *Semiconductors and Semimetals*, edited by R. K. Willardson and A. C. Beer (Academic, New York, 1972), Vol. 8, p. 370.
- ¹⁵D. Drews, A. Schneider, T. Werninghaus, A. Behres, M. Heuken, K. Heime, and D. R. T. Zahn, *Appl. Surf. Sci.* **123–124**, 746 (1998).
- ¹⁶K. Huang and A. Ruys, *Proc. R. Soc. London, Ser. A* **204**, 406 (1950).
- ¹⁷R. A. Street, T. M. Searle, and I. G. Austin, in *Amorphous and Liquid Semiconductors*, edited by J. Stuke and W. Brenig (Taylor & Francis, London, 1974), p. 953.
- ¹⁸R. W. Collins and W. Paul, *Phys. Rev. B* **25**, 5257 (1982).
- ¹⁹W. Pötz and D. K. Ferry, *Phys. Rev. B* **31**, 968 (1985).
- ²⁰M. Ramsteiner, P. Kleinert, K. H. Ploog, J. Oh, M. Konagai, and Y. Takahashi, *Appl. Phys. Lett.* **67**, 647 (1995).
- ²¹J. H. Oh, J. Shirakashi, F. Fukuchi, M. Konagai, T. Azuma, and K. Takahashi, Proceedings of the Indium Phosphide Related Materials, 1995 (unpublished), p. 797.